Available online at www.sciencedirect.com
ScienceDirect
Catalysis Today 118 (2006) 24–31
CATALYSIS TODAY
www.elsevier.com/locate/cattod

Effects of surface activity, defects and mass transfer on hydrogen permeance and *n*-value in composite palladium-porous stainless steel membranes

Federico Guazzone, Erik Edwin Engwall [1], Yi Hua Ma *

Center for Inorganic Membrane Studies, Department of Chemical Engineering, Worcester Polytechnic Institute, 100 Institute Road, Worcester, MA 01609, USA

Available online 25 July 2006

Abstract

The H_2 permeance of composite palladium-porous stainless steel (Pd-PSS) membranes was determined: (1) by assuming Sieverts' law ($n = 0.5$) and (2) by performing a non-linear fit in order to obtain the hydrogen permeance and the *n*-value. For all membranes (thickness > 15 μm) the *n*-value was higher than 0.6 at low temperatures (<350 °C) and close to 0.5 at higher temperatures (>400 °C). The activation of the membrane with the surface either seeded with palladium or oxidized in air at 350 °C for 48 h led to lower *n*-values indicating that the surface reaction rate even in thick membranes with selectivities (H_2/He) above 400 might still contribute, though to a minor extent, to the overall hydrogen permeation mechanism. For leaky membranes (selectivity $\ll 400$) the Knudsen diffusion and viscous flow of molecular H_2 through the defects led to *n*-values as high as 0.75 at 500 °C. *n*-Values higher than 0.5 were also found for Pd-PSS membranes when the PSS support had a large resistance.

Keywords: *n*-Value; Hydrogen permeance; Hydrogen flux; Palladium membranes; Surface poisoning; Leaks; Selectivity

1. Introduction

The use of composite palladium and palladium alloy membranes coupled with steam reforming of hydrocarbons in a single reaction/separation unit operation is one of the most attractive technologies for hydrogen production [1–3]. Several membrane reactor studies have shown the feasibility of methane steam reforming at temperatures ranging from 500 to 650 °C [2–5]. Membrane reactors for methanol steam reforming at 300–400 °C were also found to be a practical route for hydrogen production [6–8]. Syngas ($CO + H_2$) production from methane dry reforming at 550–650 °C using palladium based membranes was also reported [9]. It has been largely accepted that hydrogen flux through palladium films (foils and supported membranes) is governed by Eq. (1):

$$J = \frac{Q_0}{L} \exp\left(-\frac{E_p}{RT} \right) (P^n_{H_2hp} - P^n_{H_2lp}) \quad (1)$$

The terms in Eq. (1) are defined in the Nomenclature. The hydrogen flux follows the Sieverts' law when the hydrogen pressure exponent *n* is equal to 0.5, which is usually valid for thick Pd films. Deviations from the Sieverts' law ($n > 0.5$) were reported for very thin membranes [10–13]. Based on a hydrogen permeation model, Ward and Dao [14] showed that at temperatures above 400 °C, *n* was equal to 0.5 for membranes thicker than 1 μm. However, *n*-values equal to 0.6–0.7 have been reported for thick palladium membranes [15,16].

For thick membranes (>1 μm), deviations from the Sieverts' law can be caused by high pressures of hydrogen. Indeed, the derivation of the Sieverts' law assumes Eq. (2) to be valid:

$$C = \kappa P^{0.5}_{H_2} \quad (2)$$

where *C* is the hydrogen concentration in palladium, κ a proportionality constant and P_{H_2} is the hydrogen pressure. However, at 200 °C, the hydrogen absorption isothermal

* Corresponding author. Fax: +1 508 831 5853.
E-mail address: yhma@wpi.edu (Y.H. Ma).
[1] Current address: Shell International Exploration and Production Inc., Westhollow Technology Center, 3333 Highway 6 South, Houston, TX 77082-3101, USA.

0920-5861/$ – see front matter © 2006 Elsevier B.V. All rights reserved.
doi:10.1016/j.cattod.2005.12.010

Nomenclature

E_p	activation energy for hydrogen permeation (J mol^{-1} or kJ mol^{-1})
F_{H_2}	hydrogen permeance derived from a single point (m^3 m^{-2} h^{-1} bar$^{-0.5}$)
F_n	hydrogen permeance derived from the least squares analysis adjusting the n-value (m^3 m^{-2} h^{-1} bar^{-n})
$F_{0.5}$	hydrogen permeance derived from the least squares analysis assuming $n = 0.5$ (m^3 m^{-2} h^{-1} bar$^{-0.5}$)
J	gas flux (mol m^{-2} s^{-1} or m^3 m^{-2} h^{-1})
L	palladium membrane thickness (m or μm)
M_i	molecular weight for i compound (kg mol^{-1})
n	n-value or hydrogen pressure exponent
P_{H_2hp}	hydrogen partial pressure in retentate, shell or high pressure side (Pa or bar), also noted as P_{shell}
P_{H_2lp}	hydrogen partial pressure in permeate, tube or low pressure side (Pa or bar), also noted as P_{tube} or P_0
Q_0	permeability of pure palladium (mol m^{-1} s^{-1} Pa^n)
r	contribution of Knudsen flow to the total leak
R	universal gas constant (8.314 J mol^{-1} K^{-1})
T	membrane temperature (at the permeate side) (K)

Greek symbols

α	Knudsen component coefficient of He leak (m^3 m^{-2} h^{-1} bar^{-1})
β	viscous component coefficient of He leak (m^3 m^{-2} h^{-1} bar^{-2})
η_i	viscosity of gas i (Pa s^{-1})

($P^{0.5}$, hydrogen loading (H/Pd)) starts to curve as the miscibility gap is approached, i.e. >0.5 bara. Therefore, determining the hydrogen pressure exponent in the 1.1–2 bara pressure range would certainly lead to $n > 0.5$ even though bulk diffusion may still be the rate-limiting step. The permeation of hydrogen through thick palladium foils was studied by Morreale et al. [17] at very high pressures, and n-values were calculated based on permeation data from four pressure ranges (1.01–1.75, 1.01–7.75, 1.0–16.00, 1.01–26.00 bara). They reported an increase in the n-values from 0.53 (the limit value) to 0.65 as the pressure range was increased.

For thick films, deviations from the Sieverts' law can also be due to a decrease in the surface reaction rate after absorption of contaminants, such as C, CO, CO_2 or hydrocarbons, on the palladium surface [18–21]. Heat treatment in air was used for contaminant removal and also led to the increase of surface area of the palladium surface [22–24]. The palladium grain size is also believed to have an important effect on the hydrogen flux or n-value [13,25,26] but this dependence has not yet been fully explored or characterized. Finally, n-values greater than 0.5 are expected in palladium membranes with defects where a large fraction of the hydrogen permeates through pinholes and dislocations via a combined Knudsen-viscous mechanism.

The primary objective of the present study was to investigate the physical significance of the exponent n in the Sieverts' equation and show experimental evidence on the relationship between the palladium surface activity and the n-value for relatively thick membranes (20–30 μm). The effects of leaks on the hydrogen flux were also studied. In addition, the effect of temperature on the n-value was experimentally examined to elucidate the change in the permeation mechanism as a function of temperature.

2. Experimental

2.1. Membrane preparation

Composite palladium-porous stainless steel (PSS) membranes were prepared using the electroless deposition method. 0.1 and 0.2 μm grade PSS supports (1.27 cm in diameter) were purchased from Mott Metallurgical Corporation. The supports were cleaned in an alkaline solution (NaOH, 45 g/l; Na_2CO_3, 65 g/l; $Na_3PO_4{\cdot}12H_2O$, 45 g/l) for grease and dirt removal, thoroughly rinsed with de-ionized water (Di-water), rinsed with acetone and dried overnight at 120 °C. After cleaning, the supports were oxidized in stagnant air at the desired temperature (400–500 °C) to produce an oxide layer as the intermetallic

Table 1
List of membranes studied in this work

Membrane	Grade (μm)	Surface (cm^2)	Oxidation temperature (°C)	Oxidation time (h)	Thickness[a] (μm)	Use
M1	0.1	8	400	10	33	Measure n-value vs. temperature (no surface modification)
M2	0.1	8	500	10	40	Palladium seeded membrane
M3	0.1	23	500	10	19	Palladium seeded surface; reactivated surface in air at 350 °C for 48 h
M4	0.2	17	500	10	37	Effect of membrane defects on the n-value
M5	0.2	17	–	–	37	Effect of membrane defects on the n-value

[a] From weight gain.

diffusion barrier [27]. The oxidized supports were activated by successive dipping in $SnCl_2$ (1 g/l, pH 2) and $PdCl_2$ (0.1 g/l, pH 2) solutions with intermediate Di-water rinses. Palladium was deposited by the electroless plating method at 60 °C. The plating solution ($Pd(NH_3)_4Cl_2{\cdot}H_2O$, 4 g/l; Na_2EDTA, 40 g/l; NH_4OH (28%), 200 ml/l; NH_2–NH_2 (1 mol/l), 5.7 ml/l) was changed every 90 min and palladium plating rates ranged between 1.2 and 2 μm/h. The thickness of the palladium layer was determined by the gravimetric method. Details of the oxidation and plating procedure may be found in previous publications [28,29].

Composite palladium membranes studied in this work are listed in Table 1. All membranes were characterized in hydrogen atmosphere at temperatures ranging from 250 to 500 °C and pressures ranging from 1.2 to 4.5 bara. Membrane M1 was characterized directly after synthesis with no surface modification and used as a reference sample. Membrane M2 was seeded with palladium crystallites before hydrogen characterization. The palladium seeding was performed by precipitating palladium from a palladium plating bath containing high hydrazine concentrations. The precipitated layer (light brown) appeared to be relatively thin since the shine from the underneath palladium surface was still visible. Membrane M3 was characterized, at the same temperatures and pressures as all other membranes, both before and after air oxidation at 350 °C for 48 h. The surface of membranes M4 and M5 was not modified before hydrogen characterization.

2.2. Hydrogen permeation system

The permeation apparatus used was similar to the one described in an earlier publication [28] and shown schematically in Fig. 1. The permeation set-up consisted of a tube furnace and a stainless steel reactor where the membrane was housed in a shell-and-tube arrangement and sealed with stainless steel and graphite ferrules. An Eurotherm 2116 temperature controller was used to control the temperature at the reactor wall and adjusted to have the desired temperature at the tube side. MKS pressure transducers were used to measure the pressure in the tube and shell side. The H_2 and He flow rates were measured using digital mass flow meters (MKS M10MB model). All the parameters including tube temperature, pressures and flow rates were logged continuously into a computer using a TBX-68T Terminal block (National Instruments) data acquisition box and NI 4351 high precision voltage meter (National Instruments). All membranes were tested using Ultra High Purity (UHP) hydrogen gas purchased from Aimtek Co.

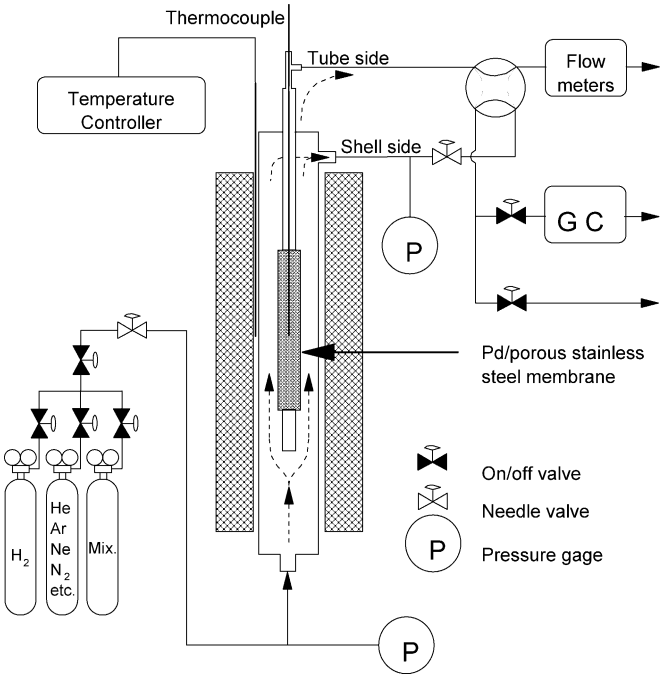

Fig. 1. Schematic diagram of the experimental set-up for permeation measurements.

2.3. Hydrogen permeance determination

The hydrogen permeance was determined by two different methods. The first method was based on the measurements of hydrogen fluxes at 20 different pressure differences (ΔP = 0.2–3.5 bar) and performing a linear regression assuming that the Sieverts' law was valid, which corresponded to assume $n = 0.5$ in Eq. (1):

$$J_{H_2} = F_{0.5}(P_{shell}^{0.5} - P_{tube}^{0.5}) \quad (3)$$

The hydrogen permeance determined assuming the Sieverts' law is denoted as $F_{0.5}$. The second method was based on a non-linear regression of the same hydrogen fluxes to determine the permeance and the n-value. Eq. (4) shows the hydrogen flux dependence on the fitted parameters: F_n and the n-value:

$$J_{H_2} = F_n(P_{shell}^{n} - P_{tube}^{n}) \quad (4)$$

The hydrogen permeance determined assuming P^n dependence of the hydrogen flux is denoted as F_n. The regression of the experimental data (linear and non-linear) was performed by the least squares method. The standard deviation for $F_{0.5}$, F_n and the n-value were 0.04, 0.2 and 0.014, respectively.

3. Results

3.1. Effect of membrane defects on the n-value

It was important to establish the minimum selectivity ($H_{2\ flux}/He_{flux}$ or H_2/He for simplicity) a composite palladium membrane should have for the n-value to remain close to 0.5. To determine this minimum selectivity, the n-value was calculated for several values of selectivity. The calculations were performed on a hypothetical Pd membrane having a hydrogen permeance equal to 10 $m^3\ m^{-2}\ h^{-1}\ bar^{-0.5}$. The selectivity values were set and ranged from 10 to 400. For each selectivity value, the He flux was calculated by Eq. (5):

$$J_{He(\Delta P)} = \frac{F_{0.5}(\Delta P^{0.5})}{\text{selectivity}} \quad (5)$$

In Eq. (5), $\Delta P^{0.5}$ stands for $P_{shell}^{0.5} - P_{tube}^{0.5}$ and the He flux was always calculated taking $P_{shell}^{0.5} = 2$ bar and $P_{tube}^{0.5} = 1$ bar. The

He flux, J_{He}, was equal to the sum of a Knudsen, α, and a viscous, βP_{ave}, contribution according to Eq. (6):

$$J_{He} = [\alpha + \beta P_{ave}]\Delta P \quad (6)$$

In order to calculate α and β, the contribution of the Knudsen flow to the overall leak had to be set. Therefore, r-values ranging from 0 (leak dominated by viscous flow) to 1 (leak dominated by Knudsen flow) were assumed for the calculations. α, β and r are given in Eq. (7):

$$r = \frac{\alpha}{\alpha + \beta P_{ave}}, \qquad \alpha = r\frac{J_{He}}{\Delta P}, \qquad \beta = \frac{J_{He}}{\Delta P}\frac{1-r}{P_{ave}} \quad (7)$$

where ΔP and P_{ave} are the pressure difference and average pressure (ΔP = 1 bar and P_{ave} = 1.5 were used in the calculations).

Having set $F_{0.5}$, the selectivity and r, α and β were calculated using Eqs. (5)–(7). The hydrogen flux was then calculated at ten different pressure differences (ΔP = 0.2–3.5 bar) according to Eq. (8):

$$J_{H_2} = F_{0.5}(\Delta P^{0.5}) + \left[\alpha\sqrt{\frac{M_{He}}{M_{H_2}}} + \beta\frac{\eta_{He}}{\eta_{H_2}}P_{ave}\right]\Delta P \quad (8)$$

where the hydrogen flux is the sum of a solution diffusion term (assuming Sieverts' law is valid), a Knudsen term and viscous term. Linear fit and non-linear fits were then performed on the calculated hydrogen flux data to determine $F_{0.5}$, F_n and the n-value.

Fig. 2 shows the n-value as a function of the selectivity (H_2/He at ΔP = 1 bar) for different values of r. The area between r = 0 and 1 curves can be denoted as the leak envelope and for any experimental point (n-value, selectivity) lying in such an envelope, its n-value could be essentially explained by the leak of the membrane. For example, from Fig. 2, the n-value of a palladium membrane with a selectivity of 400 and r = 0 is 0.52. Therefore, it can be concluded that when the selectivity of a membrane is above 400, leaks do not have any significant effect on either hydrogen permeance or n-value. In other words if $n > 0.50$ and the selectivity is higher than 400 the reasons for $n > 0.5$ are due to factors other than pinholes and imperfections.

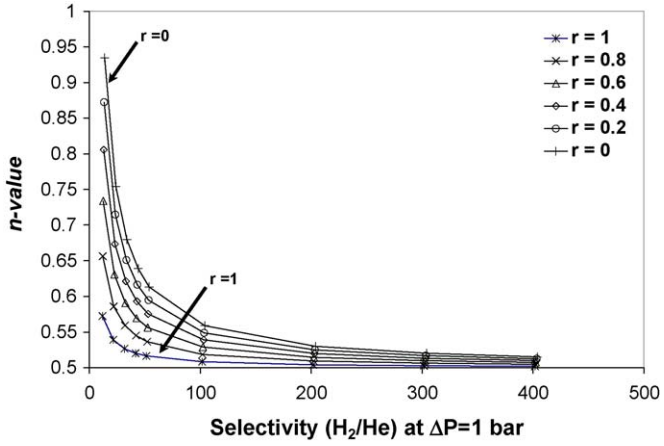

Fig. 2. n-Value as a function of selectivity for different values of r (ratio of the contribution of the Knudsen diffusion to the overall leak).

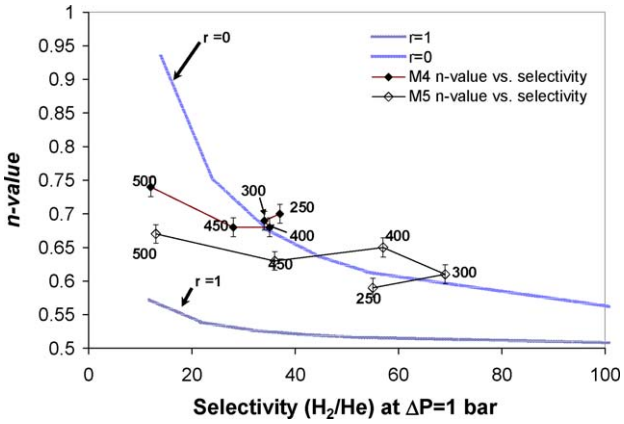

Fig. 3. n-Value as a function of selectivity of membranes M4 and M5.

In order to understand the effect of membrane defects on the hydrogen permeation and to also validate the n-value/selectivity model, two composite palladium membranes, M4 and M5, with large defects were studied. The He leak and selectivities were determined at each temperature after changing from hydrogen to helium. Fig. 3 shows the n-value as a function of the selectivity for membranes M4 and M5. Each experimental point corresponds to the temperature shown next to the point. It can be seen that all experimental data points lie very close or within the leak envelope. When selectivities were in the range of 10–20, the higher n-values could be attributed to the flow through the large pinholes in the palladium layer.

3.2. Hydrogen permeance and n-value

Fig. 4 shows the hydrogen flux at 300 °C for membrane M1 as a function of the Sieverts' driving force ($\sqrt{P} - \sqrt{P_0}$). Assuming that the Sieverts' law is valid, the slope of the line then gives the hydrogen permeance of 6.83 $m^3\ m^{-2}\ h^{-1}\ bar^{-0.5}$. Residuals ($H_{2\ exp\ flux} - H_{2\ calc\ flux}$) are also plotted as a function of the Sieverts' driving force in Fig. 4 (squares) and showed a

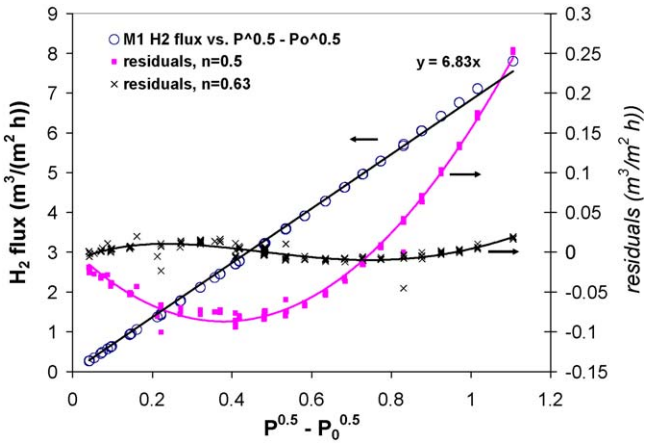

Fig. 4. Hydrogen flux as a function of $\sqrt{P} - \sqrt{P_0}$ at 300 °C for membrane M1.

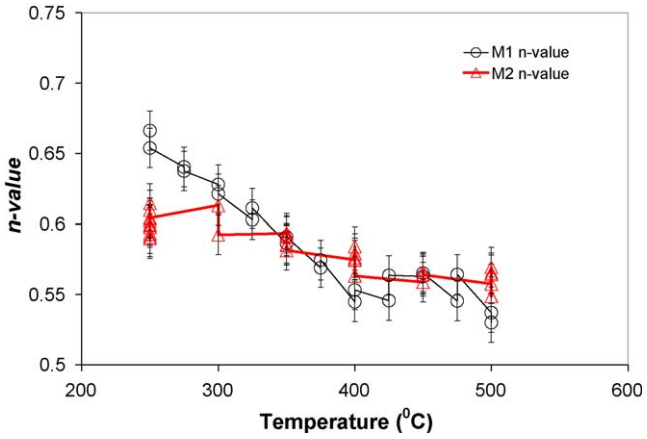

Fig. 5. *n*-Value as a function of temperature for membranes M1 and M2.

distinctive polynomial trend. In fact, the same trend was found at all temperatures at which all membranes were tested, indicating that the Sieverts' law was not followed and that the pressure exponent *n* was different from 0.5. Adjusting the *n*-value resulted in a hydrogen permeance equal to 5.0 $m^3\ m^{-2}\ h^{-1}\ bar^{-0.63}$ and an *n*-value equal to 0.63. The residuals (crosses in Fig. 4) lie very close to the value of zero indicating a better fit. The *n*-values for membrane M1 are plotted in Fig. 5 as a function of the temperature.

At 250 °C the *n*-value was equal to 0.66 and decreased to 0.55 at 400 °C. At temperatures above 400 °C the *n*-value slightly increased up to 0.57 at 450 °C and decreased again to 0.53 at 500 °C. In fact, at temperatures higher than 400 °C the *n*-value was considered as constant with a value equal to 0.53.

3.3. Effect of palladium catalytic surface modifications on the n-value

In order to accelerate the hydrogen dissociation reaction on the surface of the palladium membrane, M2 was seeded with palladium crystallites. After palladium seeding, the color of the membrane appeared brown due to the light scattering of small palladium crystallites on the surface. *n*-Values lower than the ones shown by M1 were expected. The *n*-value as a function of temperature for membrane M2 together with the *n*-values for membrane M1 is shown in Fig. 5. In the temperature range 250–350 °C the *n*-values of membrane M2 equaled 0.60 ± 0.01 and were therefore, as expected, slightly lower than the *n*-values of membrane M1 in the same temperature range. Above 350 °C, the *n*-values of M2 membrane decreased very slowly (remained almost constant) as the temperature was increased with values similar to the *n*-values of M1. Both membranes showed similar *n*-values at 500 °C (0.54 ± 0.01). After exposure to hydrogen at high temperatures, the color of the palladium film appeared very bright indicating the growth or sintering of palladium crystallites of the original thin spongy seeded layer.

The second method used to increase the rate of hydrogen dissociation on the catalytic surface of palladium was the oxidation in stagnant air at 350 °C for 48 h, which was applied on membrane M3 after the first characterization. That is, the freshly prepared membrane M3 was characterized at all temperatures from 250 to 500 °C following the same characterization procedure as M1 and M2. After the first characterization was completed, the membrane was removed from the reactor, activated and palladium plated (1.5 μm) to repair the small leak that developed during the first characterization. After the additional 1.5 μm of palladium was plated, palladium seeds were deposited using the same procedure as on membrane M2. The membrane was then oxidized in air at 350 °C for 48 h. The surface of membrane M3 after air cleaning/activation was slightly purple and not shining. At 350 °C in air PdO formed in a hill and valley pattern [22]. The color of PdO being green, the change in color from silver to slightly purple was due to the change in surface roughness and the different way light was scattered from that surface. The surface activity was related to the increase in the surface area upon oxidation [24]. Also oxidation at 350 °C cleaned the surface by burning organic contaminants from the surface. Membrane M3 was then characterized at temperatures ranging from 250 to 500 °C. The hydrogen permeance based on Sieverts' driving force at 250 °C at the

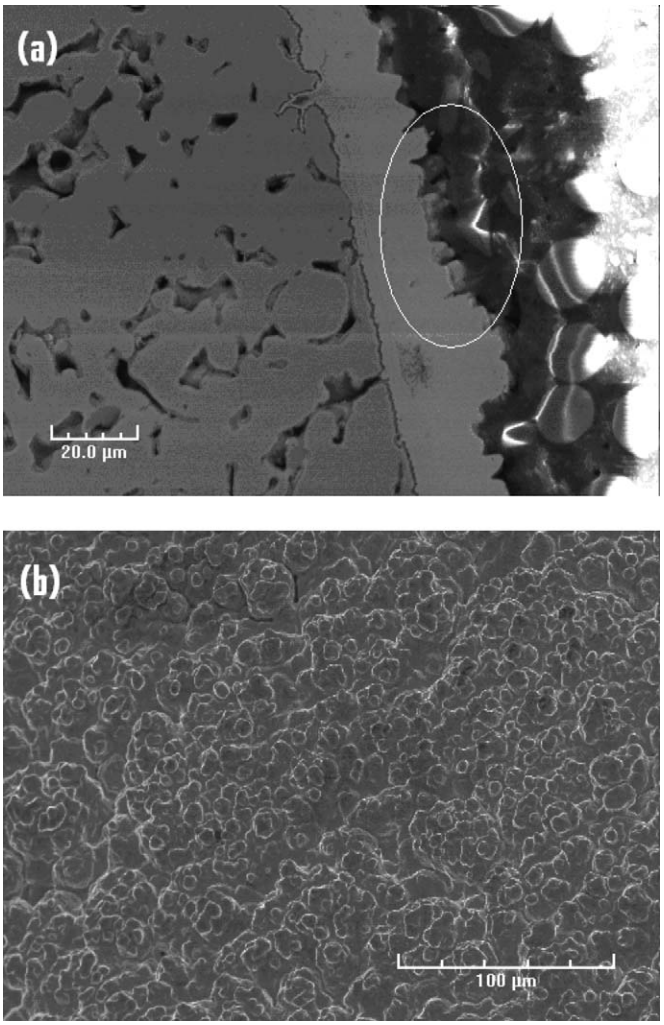

Fig. 6. Cross section (a) and surface analysis (b) of membrane M3 after hydrogen characterization.

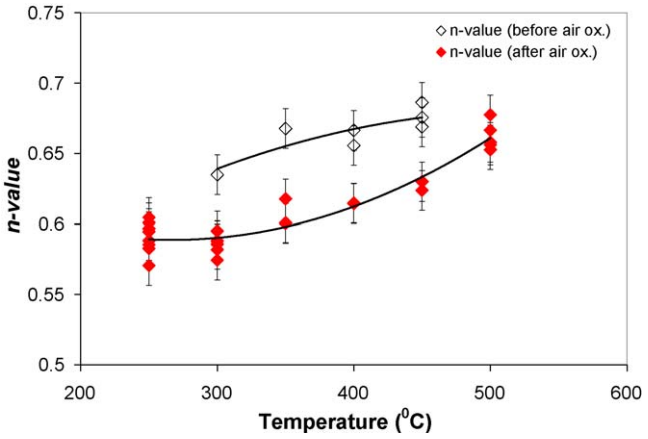

Fig. 7. *n*-Value as a function of temperature for membrane M3 before and after air oxidation. Lines through the experimental points are to assist the readers to observe the trend.

end of the first characterization was equal to 6.5 $m^3\ m^{-2}\ h^{-1}\ bar^{-0.5}$. Even though more palladium was added on M3, the hydrogen permeance at 250 °C in the second characterization equaled to 8.3 $m^3\ m^{-2}\ h^{-1}\ bar^{-0.5}$ after 200 h in hydrogen, which was higher than the hydrogen permeance at 250 °C at the end of the first characterization by 28%. Fig. 6(a) and (b) shows the cross section and the surface morphology, respectively, for membrane M3 after the second hydrogen characterization. The oxidation in air led to the formation of hills and valleys, encircled in Fig. 6(a) and seen from the top in (b), similar to the ones reported in the literature [22,23]. The formation of hills and valleys resulted in a membrane with higher hydrogen flux than the fresh palladium membrane.

During the first characterization the *n*-values for M3 ranged between 0.64 and 0.68 over the entire studied temperature range (300–500 °C) as shown in Fig. 7. After palladium plating and surface reactivation, the *n*-value of M3 during the second characterization was equal to 0.58 at 250 °C similar to the *n*-value shown by membrane M2 at 250 °C. However the *n*-values of membrane M3 increased from 0.58 at 250 °C up to 0.66 at 500 °C. At the end of the experiment the *n*-values at 500 °C had the same values as the *n*-values during the first characterization. A change in membrane color was also noticed for membrane M3 after exposure to high temperatures in hydrogen atmosphere. The surface of the membrane changed from purple after oxidation to silver color (palladium color) with little shine.

4. Discussion

Pressure exponents (*n*-values) higher than 0.5 are expected when the rate of the hydrogen dissociation reaction on the catalytic surface of the membrane is slower than or has the same order of magnitude as the rate of hydrogen bulk diffusion through the metal layer. The thickness of membrane M1 was 33 μm and normally one would have expected the hydrogen flux of M1 to follow the Sieverts' law at all temperatures since a thickness of 1 μm has been considered by many authors to be the critical thickness where the hydrogen desorption reaction became the rate-limiting step for the hydrogen permeation. However, Fig. 5 shows two temperature regions: the 250–400 °C temperature interval was characterized by a fast decrease in the *n*-value while the second temperature window 400–500 °C was characterized by a rather constant *n*-value. The decrease in the *n*-value seen in the 250–400 °C range might have been due to the increase in surface reaction rate as the temperature was increased. The decrease in *n*-value could also have been due to the thermodynamic effects. Indeed, the Pd–H phase diagram shows linear absorption isotherms (hydrogen loading, H/Pd, as a function of $P^{0.5}$) in a narrow pressure range, 0–ca. 0.1 bara, for all temperatures above 200 °C, although the applicable pressure range for a linear relation increases with increasing temperature. For instance, at 400–500 °C, the H/Pd loading as a function of $P^{0.5}$ could be considered linear in the 0–ca. 5 bara. At temperatures higher than 400 °C the pressure exponent was very close to 0.5 as shown in Fig. 5. Theoretically the *n*-value at 500 °C should have been equal to 0.5 (Sieverts' law) however, pinholes or imperfections might have formed at high temperatures leading to Knudsen and viscous flow. Indeed, the selectivity (H_2/He) of membrane M1 was just above 100 at the end of the characterization. Therefore, since the selectivity was lower than 400, and according to Fig. 2, the leak contribution to the *n*-value was not negligible. Pinholes and cracks might have resulted from the sintering of palladium clusters at high temperatures (400–450 °C) and/or stresses in the palladium layer due to the mismatch in thermal expansion coefficient between the palladium layer and the support.

In the 250–400 °C temperature range, pinhole formation was improbable, therefore, deviation from the Sieverts' law at temperatures lower than 400 °C could be attributed to: non-linear hydrogen absorption isotherm ($T < 400$ °C and 1.1–4.5 bara pressure range), contaminants adsorbed on the surface, small grain sizes, small cluster sizes and possibly mass transfer resistance in the support. Organic contaminants from the Pd plating bath (EDTA, ammonia or inorganic salts) may remain adsorbed on the surface of the membrane.

The decrease in the *n*-values seen for membrane M1 in the 250–400 °C temperature range has also been reported by several authors. Decreasing in the *n*-values from 0.62 at 450 °C to 0.55 at 600 °C were reported on composite Pd–alumina membranes [16]. The decrease in the *n*-value was attributed to the removal of surface contaminants present on the fresh surface of the membrane. However, the *n*-values reported in the same work [16], were higher than the *n*-values seen in membrane M1 at 450 °C due to the wider pressure range considered (up to 24 bar). The highest pressure considered in our work to determine the *n*-value was 4.5 bara in the feed stream and according to our calculations the relation ($P^{0.5}$, H/Pd) is linear in the 0–4.5 bara pressure range at temperatures higher than 350–400 °C. Therefore, we believe that for membrane M1, the main cause for the *n*-values to be higher than 0.5 in the 250–400 °C was due to hydrogen pressures effects and the adsorbed surface contaminants.

In order to increase the catalytic activity of the surface two different treatments of the membrane were performed: deposition of palladium seeds and oxidation at 350 °C for 48 h. Membrane M2 showed at low temperatures (250–

300 °C) lower *n*-values than membrane M1 indicating an increase of the surface reaction rate. At temperatures higher than 350 °C both membranes had similar *n*-values. Therefore, palladium seeds were only effective for increasing the surface reaction rate at low temperatures. At 300–350 °C and higher temperatures palladium grains included in the spongy catalytic layer grew and lost their hydrogen dissociative capabilities.

The reactivation by the surface oxidation at 350 °C also increased the reaction rate at the surface. During hydrogen characterization at low temperatures (250–300 °C), the thin PdO layer at the surface of the Pd membrane was reduced most probably leading to the formation of Pd nanocrystals, which were very active for the hydrogen dissociation reaction at low temperatures. At high temperatures, the Pd nanocrystals sintered with the initial Pd layer. The reduction of the thin PdO layer led to the change in color from purple after oxidation to silver color after characterization. The lack of shine was due to the roughness (hills and valleys) of the surface still present after oxidation (see Fig. 6(b)). After the surface oxidation the *n*-value of membrane M3 at 250 °C were slightly lower than the *n*-values shown by membrane M2. Also the *n*-values shown by membrane M3 during the second characterization were lower than the *n*-values shown during the first characterization. However, the *n*-value increased as a function of temperature during both permeation experiments (first and second). The increase in the *n*-value could not be explained by an increase in hydrogen flowing through the defects. Indeed, the He leak of M3 at 500 °C was 2.63×10^{-3} m^3 m^{-2} h^{-1} bar^{-1}, which corresponded to a selectivity (H_2/He) over 400 at all temperatures. A deactivation of the surface similar to M2 membrane might have happened. The support resistance may have contributed to the overall hydrogen permeation resistance of membrane M3. Indeed, the helium permeance of the bare supports for membranes M1, M2, and M3 was 207, 176 and 60 m^3 m^{-2} h^{-1} bar^{-1}, respectively. The considerably lower helium permeance for M3 is consistent with the assertion that the support resistance contributed to the high *n*-value for M3.

A mathematical model, being developed in our laboratory, predicted increasing *n*-values as the temperature was increased when the support resistance has a given contribution to the overall mass transport. As the temperature was increased, the hydrogen flux increases leading to a higher resistance in the support side. Hence, increasing the *n*-values during first and second characterization was consistent with the model (see Fig. 7) and attested to the importance of mass transport in the case of M3 membrane. Also, the mass transport resistance effect on the *n*-value was more pronounced for membrane M3 as a result of its being considerably thinner than both M1 and M2, see Table 1. Membranes M1 did not show signs of support resistance since the *n*-value at 500 °C (0.53) was close to 0.5. Moreover, the *n*-value of membrane M1 decreased as the temperature was increased. The slight deviation from 0.5 (+0.03) could be explained by the effect of the low (H_2/He) selectivity of M1 at 500 °C (∼100). Membrane M2 did not show signs of support resistance either, since the *n*-value decreased as the temperature was increased although the final *n*-value of M2 at 500 °C (0.56) was higher than 0.5.

Membranes M2 and M3 clearly showed that palladium seeding and air cleaning/oxidation increased the surface reaction rate. Therefore, even if the bulk diffusion was the main resistance for hydrogen permeation, surface reaction could still contribute, though in a reduced extent, to the transport of hydrogen. The surface reaction even had a more pronounced resistance at lower temperatures mainly due to the presence of impurities adsorbed on the palladium surface. Impurities could be removed by heating (*n*-value decreasing with temperature) and air oxidation at 300–350 °C.

5. Conclusion

The hydrogen permeance of composite Pd-PSS membranes was determined using two methods: assuming the Sieverts' law ($n = 0.5$) and performing a non-linear regression on the experimental data to determine the *n*-value and the permeance. The *n*-value of a fresh palladium membrane (with no surface modification) decreased from 0.67 to 0.53 as temperature was raised from 300 to 500 °C indicating the removal of contaminants and the increase of the linearity region of the isotherm of the $P^{1/2}$ versus *n*(H/Pd) as temperature was increased. Defects in the dense Pd layer caused the *n*-value to deviate from 0.5 at 500 °C. Surface activation by palladium seeding or air oxidation at $T > 300$ °C slightly increased the rate of hydrogen absorption/desorption reactions. The activity of the freshly formed palladium activated surface decreased due to palladium crystallites sintering at high temperatures. The model prediction validated by experimental data showed that the effect of leak on the *n*-value was negligible if the selectivity of the membrane was over 400.

Acknowledgements

The authors gratefully acknowledge the financial support provided by Shell International Exploration and Production Inc. and Shell Hydrogen. Diana M. Otálvaro is gratefully acknowledged for the preparation of some of the composite Pd-PSS membranes and her outstanding knowledge in SEM sample preparation.

References

[1] O.Y. Shirasaki, Y. Otha, K. Kobayashi, K. Kuroda, in: Proceedings of the 27th Annual Meeting of Japan Petroleum Institute on Development of a Hydrogen Separation Reformer, 1997, p. 247.
[2] S.L. Wellington, A.N. Matzakos, T. Mikus, M.J. Ward, US Patent 0,068,260 (2003).
[3] A.N. Matzakos, S.L. Wellington, T. Mikus, M.J. Ward, US Patent 0,068,269 (2003).
[4] E. Kikuchi, Y. Nemoto, M. Kajiwara, S. Uemiya, T. Kojima, Catal. Today 26 (2000) 75.
[5] N. Itoh, Y. Kaneko, A. Igarashi, Ind. Eng. Chem. Res. 41 (2002) 4702.
[6] Y.M. Lin, G.L. Lee, M.H. Rei, Catal. Today 44 (1998) 343.
[7] Y.M. Lin, M.H. Rei, Int. J. Hydrogen Energy 25 (2000) 211.
[8] Y.M. Lin, M.H. Rei, Catal. Today 67 (2001) 77.

[9] J. Galuszka, R.N. Pandey, S. Ahmed, Catal. Today 46 (1998) 83.
[10] A.L. Athayde, R.W. Baker, P. Nguyen, J. Membr. Sci. 94 (1994) 299.
[11] V. Jayaraman, Y.S. Lin, J. Membr. Sci. 104 (1995) 241.
[12] S.E. Nam, S.H. Lee, K.H. Lee, J. Membr. Sci. 153 (1999) 163.
[13] B.A. McCool, Y.S. Lin, J. Mater. Sci. 36 (2001) 3221.
[14] T.L. Ward, T. Dao, J. Membr. Sci. 153 (1999) 211.
[26] S. Yan, H. Maeda, K. Kusakabe, S. Morooka, Ind. Eng. Chem. Res. 33 (1994) 616.
[15] R.C. Hurlbert, J.O. Konecny, J. Chem. Phys. 34 (1961) 655.
[16] J.P. Collins, J.D. Way, Ind. Eng. Chem. Res. 32 (1993) 3006.
[17] B.D. Morreale, M.V. Ciocco, R.M. Enick, B.I. Morsi, B.H. Howard, A.V. Cugini, K.S. Rothenberger, J. Membr. Sci. 212 (2003) 87.
[18] S. Tosti, L. Bettinali, S. Castelli, F. Sarto, S. Scaglione, V. Violante, J. Membr. Sci. 196 (2002) 241.
[19] J.N. Keuler, L. Lorenzen, J. Membr. Sci. 195 (2002) 203.
[20] J.K. Ali, E.J. Newson, D.W. Rippin, J. Membr. Sci. 89 (1994) 171.
[21] K. Yamakawa, M. Ege, B. Ludescher, M. Hirscher, J. Alloys Compd. 352 (2003) 57.
[22] S. Aggarwal, A.P. Monga, S.R. Perusse, R. Ramesh, V. Ballarotto, E.D. Williams, B.R. Chalamala, Y. Wei, R.H. Reuss, Science 287 (2000) 2235.
[23] F. Roa, D. Way, ACS Fuel Chem. Div. Preprints 48 (2003) 335.
[24] J. Han, G. Zhu, D. Zemlyanov, F.H. Ribeiro, J. Catal. 225 (2004) 7.
[25] K.J. Bryden, J.Y. Ying, J. Membr. Sci. 203 (2002) 29.
[26] S. Yan, H. Maeda, K. Kusakabe, S. Morooka, Ind. Eng. Chem. Res. 33 (1994) 616.
[27] Y.H. Ma, P.P. Mardilovich, Y. She, US Patent 6,152,987.
[28] P.P. Mardilovich, Y. She, Y.H. Ma, M.H. Rei, AIChE J. 44 (1998) 310.
[29] Y.H. Ma, B.C. Akis, M.E. Ayturk, F. Guazzone, E.E. Engwall, I.P. Mardilovich, Ind. Eng. Chem. Res. 43 (2004) 2936.